Cochaperone Mzb1 is a key effector of Blimp1 in plasma cell differentiation and β1-integrin function

Virginia Andreani[a], Senthilkumar Ramamoorthy[a], Abhinav Pandey[a], Ekaterina Lupar[a], Stephen L. Nutt[b,c], Tim Lämmermann[a], and Rudolf Grosschedl[a,1]

[a]Department of Cellular and Molecular Immunology, Max Planck Institute of Immunobiology and Epigenetics, 79108 Freiburg, Germany; [b]The Molecular Immunology Division, The Walter and Eliza Hall Institute of Medical Research, Parkville, VIC 3052, Australia; and [c]Department of Medical Biology, University of Melbourne, Parkville, VIC 3010, Australia

Edited by Klaus Rajewsky, Max Delbrück Center for Molecular Medicine, Berlin, Germany, and approved September 4, 2018 (received for review June 6, 2018)

Plasma cell differentiation involves coordinated changes in gene expression and functional properties of B cells. Here, we study the role of Mzb1, a Grp94 cochaperone that is expressed in marginal zone (MZ) B cells and during the terminal differentiation of B cells to antibody-secreting cells. By analyzing *Mzb1*$^{-/-}$*Prdm1*$^{+/gfp}$ mice, we find that Mzb1 is specifically required for the differentiation and function of antibody-secreting cells in a T cell-independent immune response. We find that Mzb1-deficiency mimics, in part, the phenotype of Blimp1 deficiency, including the impaired secretion of IgM and the deregulation of Blimp1 target genes. In addition, we find that *Mzb1*$^{-/-}$ plasmablasts show a reduced activation of β1-integrin, which contributes to the impaired plasmablast differentiation and migration of antibody-secreting cells to the bone marrow. Thus, Mzb1 function is required for multiple aspects of plasma cell differentiation.

Mzb1 | Grp94 | Blimp1 | integrin | plasma cell

The terminal differentiation of B cells into antibody-secreting cells (ASCs) is an essential process in the humoral immune response. After an encounter with antigen, B cells proliferate and differentiate into short-lived, cycling plasmablasts (PBs) that secrete antibody and reside in extrafollicular foci of secondary lymphoid organs (1). PBs can further differentiate into quiescent long-lived plasma cells (PCs) after migration to the bone marrow (BM), which provides niches that enable PC longevity (2). However, the majority of PCs are derived from activated B cells that enter the B cell follicles of secondary lymphoid organs and form germinal centers (GC) under the influence of follicular T helper cells. After extensive proliferation and affinity maturation of the B cell receptor, GC B cells differentiate into long-lived PCs or memory B cells (2).

Mature B cells include the innate-like marginal zone (MZ) B cells, B1 cells, and the dominant follicular B (Fo B) cell subset (3). MZ B and B1 cells respond rapidly to T cell-independent (TI) antigens, such as bacterial lipopolysaccharides (LPS), but they can also engage in a slower T cell-dependent (TD) immune response that is mediated primarily by Fo B cells. The generation of ASCs in a TD response involves an initial extrafollicular response step that produces PB and a subsequent GC response step that produces PC and memory B cells (4). ASCs expand their endoplasmic reticulum (ER) as a consequence of the unfolded protein response (UPR) that is induced by protein overloading and results in the activation of the transcription factor XBP-1, which regulates the UPR and secretion of immunoglobulins (Ig). The UPR can consequently regulate the folding, processing, and export of the new synthetized proteins (5, 6). Before the activation of the UPR and XBP-1, the transcription factor IRF4 initiates PB differentiation by the activation of the *Prdm1* gene, encoding the transcription factor Blimp1 (7). Blimp1 silences the expression program of B cells and contributes to the activation of genes involved in the regulation of the UPR and the migratory and sessile properties of PBs and PCs (8, 9).

The *Mzb1* (*pERp1*) gene, which encodes a B cell-specific and ER-localized protein, is abundantly expressed in MZ B cells and B1 cells, and its expression increases to even higher levels during differentiation of activated B cells to ASCs (10–14). Mzb1 functions as a cochaperone of the substrate-specific chaperone Grp94/gp96 (Hsp90b1) under ER stress conditions and enables efficient antibody secretion in vitro and in immunized mice (12, 13). Mzb1 and Hsp90b1 are also among the few genes that are bound and activated by Blimp1 during the B cell to preplasmablast (pre-PB) transition (8). Mzb1 has also been implicated in the activation of integrin β1, which forms a heterodimer with the α4-integrin to bind vascular cell adhesion molecule (VCAM)-1 and to mediate lymphocyte adhesion and migration (12, 15, 16). VCAM-1 is abundantly expressed in the red pulp of the spleen and facilitates integrin-mediated B cell localization in the splenic MZ and peripheral lymphoid tissue compartmentalization (17, 18). In addition, the expression of VCAM-1 in BM stromal cells is important for the maturation and retention of PCs in the BM (19–23).

Previously, the role of Mzb1 has been studied primarily in cell cultures and has focused on the secretion of antibodies. Therefore, questions arise as to whether and how the highly abundant expression of *Mzb1* in ASCs regulates the terminal differentiation of

Significance

Antibody-secreting plasma cells are effectors of the humoral immune response. Transcription factor Blimp1 (Prdm1) is essential for the generation and function of plasma cells, and it regulates many genes, including *Mzb1* (*pERp1*). Mzb1 protein is localized in the endoplasmic reticulum and acts as a cochaperone for the substrate-specific chaperone Grp94 (gp96). By the analysis of *Mzb1*$^{-/-}$*Prdm1*$^{+/gfp}$ mice, we find that Mzb1 is required for T cell-independent immune responses and differentiation of plasma cells. In *Mzb1*$^{-/-}$*Prdm1*$^{+/gfp}$ mice, we also observe impaired β1-integrin activation and trafficking of plasma cells to the bone marrow. Notably, we show that Mzb1 accounts for many of the Blimp1-associated downstream functions, suggesting that Mzb1 is a key effector of the Blimp1 regulatory network in plasma cells.

Author contributions: V.A., T.L., and R.G. designed research; V.A., A.P., and E.L. performed research; V.A., S.R., A.P., S.L.N., T.L., and R.G. analyzed data; and V.A. and R.G. wrote the paper.

The authors declare no conflict of interest.

This article is a PNAS Direct Submission.

Data deposition: The data reported in this paper have been deposited in the Gene Expression Omnibus (GEO) database, https://www.ncbi.nlm.nih.gov/geo (accession no. GSE118124).

[1]To whom correspondence should be addressed. Email: grosschedl@ie-freiburg.mpg.de.

This article contains supporting information online at www.pnas.org/lookup/suppl/doi:10.1073/pnas.1809739115/-/DCSupplemental.

Published online September 26, 2018.

B cells, the function of integrins, and the trafficking of ASCs in vivo. Here, we show that Mzb1 is required for productive TI antibody responses and for differentiation of PBs and PCs. We find that many Blimp1 target genes are de-regulated in *Mzb1* knockout cells, suggesting a positive feedback loop between Blimp1 and its effector gene *Mzb1*. In addition, we find that the function of Mzb1 in the activation of β1-integrin affects the migratory properties of ASCs and their trafficking and retention to the BM.

Results

Impaired TI PC Differentiation in *Mzb1*$^{-/-}$*Prdm1*$^{+/gfp}$ Mice. With the aim of gaining insight into the role of Mzb1 in PC differentiation and function, we crossed *Mzb1*$^{-/-}$ mice with *Prdm1*$^{+/gfp}$ reporter mice that allow for the identification and separation of short-lived, cycling Blimp1^{int} PBs and long-lived, quiescent Blimp1^{hi} PCs (24). To assess the role of Mzb1 in the TD PC generation, we immunized *Mzb1*$^{-/-}$*Prdm1*$^{+/gfp}$ and *Mzb1*$^{+/+}$*Prdm1*$^{+/gfp}$ littermates with (4-hydroxy-3-nitrophenyl)acetyl–keyhole limpet hemocyanin (NP-KLH) and analyzed the frequencies of ASCs in spleen and BM by flow cytometry at 7 d postimmunization (dpi). Similar frequencies of Blimp1-GFP^{int} PBs and Blimp1-GFP^{hi} PCs were detected in the spleen and BM of *Mzb1*$^{-/-}$*Prdm1*$^{+/gfp}$ mice relative to *Mzb1*$^{+/+}$*Prdm1*$^{+/gfp}$ mice (Fig. 1 *A* and *B*). Moreover, we found that the Mzb1 deficiency had no significant effect on PC differentiation in vitro, driven by CD40L, IL-4, and IL-5 (*SI Appendix*, Fig. S1 *A* and *B*). We also did not detect any significant difference in the generation of GC B cells in *Mzb1*$^{-/-}$ and *Mzb1*$^{+/+}$ mice after immunization with NP-KLH

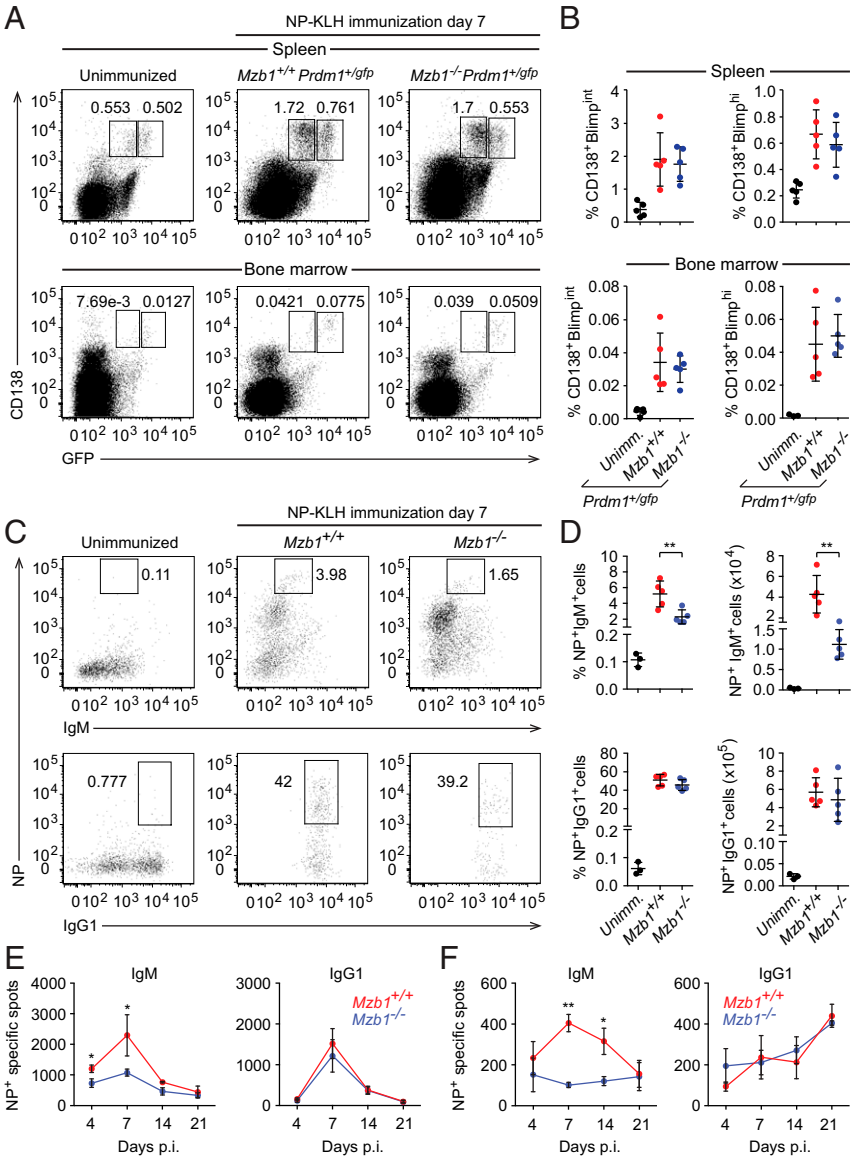

Fig. 1. Impaired IgM secretion in TD-immune responses of *Mzb1*$^{-/-}$ mice. (*A*) Flow cytometry to identify CD138^{+}Blimp-GFP^{+} cells in spleen (*Upper*) and BM cells (*Lower*) from *Mzb1*$^{+/+}$*Prdm1*$^{+/gfp}$ and *Mzb1*$^{-/-}$ *Prdm1*$^{+/gfp}$ mice at 7 dpi with NP-KLH. Numbers represent cell frequencies. (*B*) Mean (±SD) frequencies of CD138^{+}Blimp-GFP^{int} and CD138^{+}Blimp-GFP^{hi} cells in spleen and BM of immunized or unimmunized mice; $n = 5$. Error bars show SD. (*C*) Flow cytometry to determine the frequencies of NP^{+}IgM^{+} cells (*Upper*) and NP^{+}IgG1^{+} cells (*Lower*) among B220^{low}CD138^{+} splenocytes of unimmunized or NP-KLH– immunized mice. (*D*) Mean (±SD) frequencies (*Left*) and numbers (*Right*) of NP^{+}IgM^{+} (*Upper*) and NP^{+}IgG1^{+} cells (*Lower*) as gated in *C*. (*E* and *F*) ELISpot analysis to detect NP-specific IgM- (*Left*) and IgG1- (*Right*) secreting cells in the spleen (*E*) and BM (*F*) of *Mzb1*$^{+/+}$ and *Mzb1*$^{-/-}$ mice at different days postimmunization; $n =$ 4 mice per genotype. Error bars show SD. $^{*}P < 0.05$, $^{**}P < 0.01$.

(*SI Appendix*, Fig. S1 *C* and *D*). However, the immunization of *Mzb1*$^{-/-}$ with NP-KLH revealed a significant decrease in the frequency of NP-specific IgM^{+} ASCs relative to *Mzb1*$^{+/+}$ mice (Fig. 1 *C* and *D*). This difference was not observed for the more abundant NP-specific IgG1^{+} ASCs (Fig. 1 *C* and *D*). ELISpot analysis showed that the secretion of NP-specific IgM antibodies in splenic and BM-derived ASCs of *Mzb1*$^{-/-}$ mice was reduced compared with *Mzb1*$^{+/+}$ mice (Fig. 1 *E* and *F*). Notably, no defect in the secretion of NP-specific IgG1 antibodies was observed in *Mzb1*$^{-/-}$ mice. Thus, Mzb1 is specifically required for the generation of IgM^{+} ASCs and proper secretion of IgM after TD immunization, but is dispensable for the generation of follicular PBs and PCs.

To assess a potential role of Mzb1 in the differentiation and function of extrafollicular PBs, we immunized *Mzb1*$^{-/-}$*Prdm1*$^{+/gfp}$ and *Mzb1*$^{+/+}$*Prdm1*$^{+/gfp}$ mice with the TI antigen trinitrophenylated derivatives of LPS (TNP-LPS) and examined the frequencies of CD138^{+}Blimp-GFP^{int} PBs and CD138^{+}Blimp1-GFP^{hi} PCs in the spleen and BM by flow cytometry at 3 dpi (Fig. 2*A*). Similar frequencies of CD138^{+}Blimp1-GFP^{int} PBs were detected in *Mzb1*$^{-/-}$*Prdm1*$^{+/gfp}$ and *Mzb1*$^{+/+}$*Prdm1*$^{+/gfp}$ mice but the frequency of CD138^{+}Blimp1-GFP^{hi} PCs was reduced in both the spleen and BM of *Mzb1*$^{-/-}$*Prdm1*$^{+/gfp}$ mice (Fig. 2 *A* and *B*). ELISpot analysis detected similar numbers of antigen-specific ASCs in the spleen of *Mzb1*$^{-/-}$*Prdm1*$^{+/gfp}$ and *Mzb1*$^{+/+}$ *Prdm1*$^{+/gfp}$ mice (Fig. 2 *C* and *D*, *Top*). However, the numbers of TNP-specific IgM^{+} ASCs were markedly reduced in the BM of *Mzb1*$^{-/-}$*Prdm1*$^{+/gfp}$ relative to those in *Mzb1*$^{+/+}$*Prdm1*$^{+/gfp}$ mice (Fig. 2 *C* and *D*, *Lower*). In comparison with *Mzb1*$^{+/+}$*Prdm1*$^{+/gfp}$ mice, immunizations of *Mzb1*$^{-/-}$*Prdm1*$^{+/gfp}$ mice with NP-Ficoll also generated fewer BM ASCs that secrete NP-specific IgG3 as a typical TI isotype (*SI Appendix*, Fig. S1 *E* and *F*). The equivalent numbers of TNP-specific ASCs in the spleen of *Mzb1*$^{+/+}$ and *Mzb1*$^{-/-}$ could be accounted for by the similar high abundance of Blimp1-GFP^{int} PBs, whereas the ASCs population in BM is dominated by the Blimp1-GFP^{hi} PCs that are diminished in *Mzb1*$^{-/-}$ mice. It is known that PCs in the BM secrete more antibodies per cell and per minute than PBs in the spleen (25). Interestingly, we also observed a decreased frequency of CD138^{+} Blimp1-GFP^{+} cells in the peripheral blood of *Mzb1*$^{-/-}$*Prdm1*$^{+/gfp}$ 3 dpi (Fig. 2*E*). This decreased frequency of cells was not due to diminished cell survival because we did not detect any differences in the apoptosis of *Mzb1*$^{-/-}$ and *Mzb1*$^{+/+}$ ASCs (Fig. 2*F*).

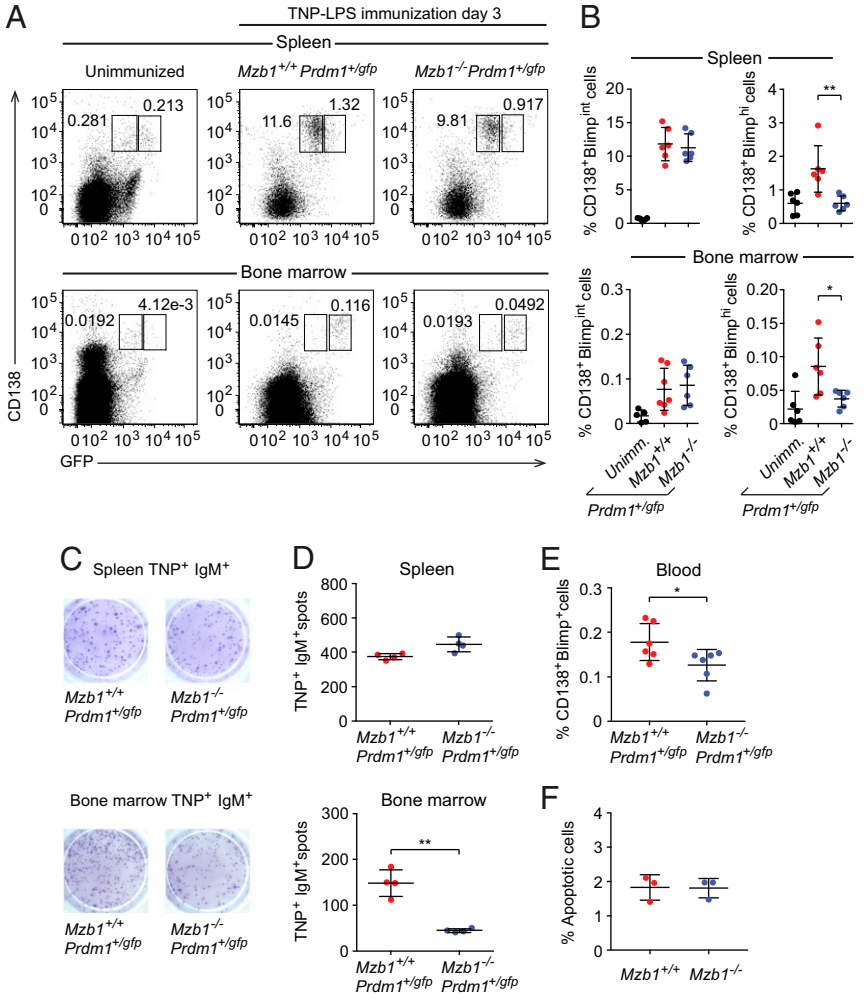

Fig. 2. Defect of PC differentiation in TI-immune responses of *Mzb1*$^{-/-}$ mice. (*A*) Flow cytometry to detect CD138^{+}Blimp-GFP^{+} cells in the spleen (*Upper*) and BM (*Lower*) of *Mzb1*$^{+/+}$*Prdm1*$^{+/gfp}$ and *Mzb1*$^{-/-}$*Prdm1*$^{+/gfp}$ mice 3 dpi with TNP-LPS. Numbers represent cell frequencies. (*B*) Mean (±SD) frequencies of *Mzb1*$^{+/+}$ and *Mzb1*$^{-/-}$ CD138^{+} *Blimp-GFP*^{int} and CD138^{+} *Blimp-GFP*^{hi} cells in the spleen and BM, as gated in *A*. Representative ELISpot (*C*) and mean (±SD) numbers (*D*) of TNP^{+}IgM^{+} CD138^{+}Blimp-GFP^{+} cells in the spleen (*Upper*) and BM (*Lower*) 3 dpi, $n = 4$. (*E*) Mean (±SD) frequencies of CD138^{+}Blimp-GFP^{+} cells in blood of TNP-LPS–immunized mice 3 dpi. (*F*) Analysis of the frequencies (±SD) of apoptotic B220^{low} CD138^{+} cells in *Mzb1*$^{+/+}$ and *Mzb1*$^{-/-}$ mice 3 dpi with TNP-LPS. Data are representative of three experiments with three to six mice per group and experiment. $^{*}P < 0.05$, $^{**}P < 0.01$.

Taken together, these data suggest that Mzb1 is required for the generation and function of PCs after TI immunization.

Transcriptome of *Mzb1*$^{-/-}$ PBs Resembles That of *Prdm1*$^{-/-}$ PBs. To gain insight into the molecular basis of the deficiency in the generation of extrafollicular PBs, we conducted an RNA-seq analysis on B220^{+} cells from the spleen of *Mzb1*$^{-/-}$*Prdm1*$^{+/gfp}$ and *Mzb1*$^{+/+}$*Prdm1*$^{+/gfp}$ mice that have been stimulated with LPS in vitro for 4 d. Similar frequencies of pre-PBs (CD138^{-} Blimp1-GFP^{+}) were detected in both Mzb1 WT and mutant cell cultures (Fig. 3*A*). In cultures from Mzb1-deficient mice, however, we observed a reduced frequency of PBs (CD138^{+} Blimp1-GFP^{+}) and increased frequency of activated B cells (Act B) (CD138^{-} Blimp1-GFP^{-}) relative to cultures from *Mzb1*$^{+/+}$ mice. The absolute numbers of *Mzb1*$^{-/-}$ pre-PBs and PBs were also reduced relative to *Mzb1*$^{+/+}$ cells (Fig. 3*B*). The block of PB differentiation correlates with the robust up-regulation of Mzb1 RNA in *Mzb1*$^{+/+}$ pre-PBs (Fig. 3*C*).

RNA-seq analysis of these cell populations identified 63 up-regulated and 20 down-regulated genes in Mzb1-deficient pre-PBs relative to *Mzb1*$^{+/+}$ pre-PBs (Fig. 3*D*). In *Mzb1*$^{-/-}$ PBs, 77 genes were up-regulated whereby 29 genes were shared between pre-PBs and PBs (Fig. 3*E*). Analysis of publicly available ChIP-seq and ATAC-seq datasets for histone modifications, transcription factor occupancy, and chromatin accessibility at the *Mzb1* gene indicated that both Blimp1 and IRF4 bind the promoter region of the *Mzb1* gene (Fig. 3*F*) (8). Moreover, the *Mzb1* gene shows accessibility already in activated B cells and enhanced histone H3 K9 acetylation in PBs (Fig. 3*F*). Notably, 18 of 77 genes that were up-regulated in *Mzb1*$^{-/-}$ PBs have been

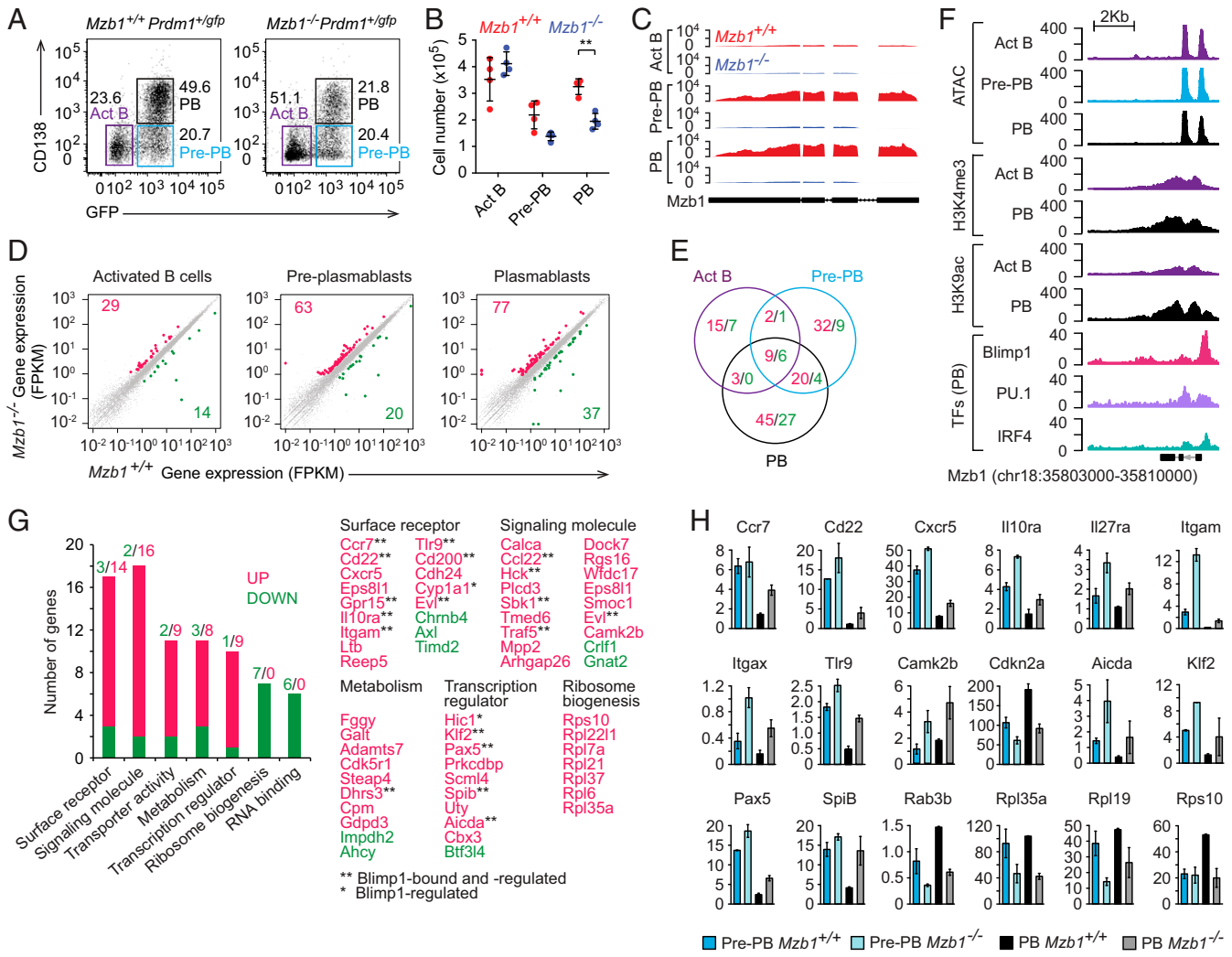

Fig. 3. Changes in the transcriptome of *Mzb1*$^{-/-}$ PBs. Flow cytometry to detect frequencies (*A*) and mean (±SD) numbers (*B*) of CD138^{-}Blimp-GFP^{-} activated B cells (Act B), CD138^{-}Blimp-GFP^{+} Pre-PB, and CD138^{+}Blimp-GFP^{+} PB at 4 d after LPS stimulation of *Mzb1*$^{+/+}$*Prdm1*$^{+/gfp}$ and *Mzb1*$^{-/-}$*Prdm1*$^{+/gfp}$ B220^{+} splenocytes. Data are representative of three experiments; $n = 4$. $^{**}P < 0.01$. (*C*) RNA-Seq reads of *Mzb1* transcripts from *Mzb1*$^{+/+}$ (red) and *Mzb1*$^{-/-}$ (blue) Act B, Pre-PB, and PB. (*D*) Scatter plot of gene-expression levels in *Mzb1*$^{+/+}$ (*x* axis) and *Mzb1*$^{-/-}$ (*y* axis) Act B cells (*Left*), Pre-PB (*Center*), PB (*Right*). The unaltered (gray), up- (red), and down-(green) regulated genes are highlighted. (*E*) Overlap of differentially expressed genes in Act B cells, Pre-PB, and PB. Numbers of up- (red) and down- (green) regulated genes in *Mzb1*$^{-/-}$ relative to *Mzb1*$^{+/+}$ are shown. (*F*) Tn5 transposase accessible (ATAC-Seq) regions, H3K4me3, and H3K9ac marks, on the *Mzb1* locus in Act B cells (purple), Pre-PB (blue), and PB (black). The occupancy of IRF4, PU.1, and Blimp1 on the *Mzb1* locus in PB cells, is shown (*Bottom*). Data source, NCBI GEO accession no. GSE71698. (*G*) Functional classification of up- (red) and down- (green) regulated genes in *Mzb1*$^{-/-}$ PB. Numbers above the bars indicate number of genes associated with each functional class. Selected genes from functional classes are indicated (*Right*). (*H*) Levels (fragments per kilobase of transcript per million mapped reads) of differentially expressed key genes in *Mzb1*$^{+/+}$ and *Mzb1*$^{-/-}$ Pre-PB and PB. Error bars show SD; $n = 2$.

previously identified as genes that are repressed by Blimp1 (8). These include genes encoding the surface receptors CCR7, CD22, IL-10Rα, Toll-like receptor 9 (TLR-9), the signaling molecules CCL2, Traf5, and the transcription factors Pax-5, Klf-2, Spi-B, and AID (Fig. 3 *G* and *H*). The majority of these and other genes were also deregulated in pre-PBs but not in Act B cells, suggesting that the Mzb1-deficiency mimics, in part, the changes in gene expression associated with Blimp1-regulated PC differentiation.

Impaired Integrin Activation and Adhesion of Mzb1$^{-/-}$ PBs and MZ B Cells. Recent studies established that Prdm1-deficiency leads to impaired migration and substrate adhesion of PB (8). Given the striking overlap in gene-expression changes between Mzb1- and Prdm1-deficiency, we next examined whether Mzb1-deficient PBs show similar deficits in their adhesive properties. Indeed, Mzb1-deficient pre-PBs and PBs showed impaired adhesion to intercellular adhesion molecule-1 (ICAM-1) and VCAM-1, which are ligands for αLβ2- and α4β1-integrins, respectively (Fig. 4*A*). However, no significant changes in the adhesion of Mzb1-deficient Act B cells were observed. Previously, we have shown that Mzb1 knockdown in the mature B cell line K46 leads to decreased chemokine-induced adhesion in vitro (12). In these cells, Mzb1 regulates chemokine-induced integrin activation by promoting the transition of the low-affinity bent conformation to the high-affinity extended conformation of integrins. To examine whether or not Mzb1 deficiency also causes altered integrin activation in PBs, we used pan-β1 antibodies to measure all forms of cell surface β1-integrin or a conformation-specific anti-β1 antibody that specifically interacts with the extended conformation of the β1-subunit (26, 27). Our flow cytometric analysis of Act B cells, pre-PBs, and PBs generated from WT and Mzb1-deficient mice showed that Mzb1-deficient pre-PBs and PBs show reduced levels of the extended form of β1 on the surface (Fig. 4*B*). In contrast, the levels of total β1-integrin remained unchanged (Fig. 4*C*). In agreement with this finding, Mzb1-deficient pre-PBs and PBs showed an impaired binding of soluble VCAM-1 (Fig. 4*D*). To examine the effects of Mzb1 deficiency on cell migration, we performed a migration assay with VCAM-1–coated transwells. This assay indicated that *Mzb1*$^{-/-}$ pre-PBs and PBs migrate less efficiently than their WT counterparts toward the chemokine CXCL12 (Fig. 4*E*). This impaired migration of Mzb1-deficient pre-PBs and PBs was not due to an altered chemokine sensing, as evidenced by the normal expression of CXCR4, the receptor for CXCL12 (Fig. 4*F*). Thus, Mzb1 is required for the activation and function of β1-integrin in pre-PBs and PBs.

Given that MZ B cells present the predominant cell type for the generation of short-lived PBs and PCs during TI-dependent immune responses (4, 28), we asked whether the genetic depletion of Mzb1 already interferes with integrin functionality in MZ B cells. Similar to the observations in pre-PBs and PBs, Mzb1-deficient MZ B cells show a reduced surface expression of the extended form of β1-integrin, relative to Mzb1-expressing MZ B cells (*SI Appendix*, Fig. S2*A*). Mzb1 low-expressing Fo B cells only show low levels of activated β1-integrin on their surface, without obvious differences between *Mzb1*$^{+/+}$ and *Mzb1*$^{-/-}$ Fo B cells (*SI Appendix*, Fig. S2*B*). Moreover, *Mzb1*$^{-/-}$ MZ B cells, but not *Mzb1*$^{-/-}$ Fo B cells, show an impaired VCAM-1–Fc binding and adhesion to VCAM-1–coated plates, in the absence or presence of CXCL12 and CXCL13 chemokines (compare *SI Appendix*, Fig. S2 *C* and *E* with *SI Appendix*, Fig. S2 *D* and *F*).

To examine whether or not the impaired expression of the extended form of β1-integrin reflects a defect in Mzb1-dependent protein folding, we performed limited trypsin digestion on *Mzb1*$^{+/+}$ and *Mzb1*$^{-/-}$ MZ B and Fo B cells. Gel electrophoretic separation of the partially digested proteins indicated that β1-integrin is degraded in Mzb1-deficient MZ B cells at lower concentrations of trypsin than in *Mzb1*$^{+/+}$ MZ B cells (Fig. 5*A*). In contrast, similar patterns of β1 degradation were observed in *Mzb1*$^{-/-}$ and *Mzb1*$^{+/+}$ Fo B cells (Fig. 5*B*). Notably, the degradation patterns of α4-integrin and CD19 were similar in both MZ B and Fo B cells from *Mzb1*$^{-/-}$ and *Mzb1*$^{+/+}$ mice. To gain some insight into the mechanism by which Mzb1 affects the conformation of β1-integrin, we examined whether Mzb1 affects the interaction between Grp94 and β1-integrin. To this end, we performed coimmunoprecipitation of lysates from WT and *Mzb1*$^{-/-}$ B1-8 B cells with anti-Grp94 antibody, followed by immunoblot analysis to detect Grp94, β1-integrin, and α4-integrin. In *Mzb1*$^{+/+}$ cells, we detected an association of Grp94 with the ~100-kD precursor form of β1, termed β1′, which is localized in the ER and is not yet associated with the α4-subunit (29) (Fig. 5*C*). In contrast, no association of the ~125-kDa mature (Golgi) form of β1 was detected in lysates from *Mzb1*$^{-/-}$ cells. Taken together, these

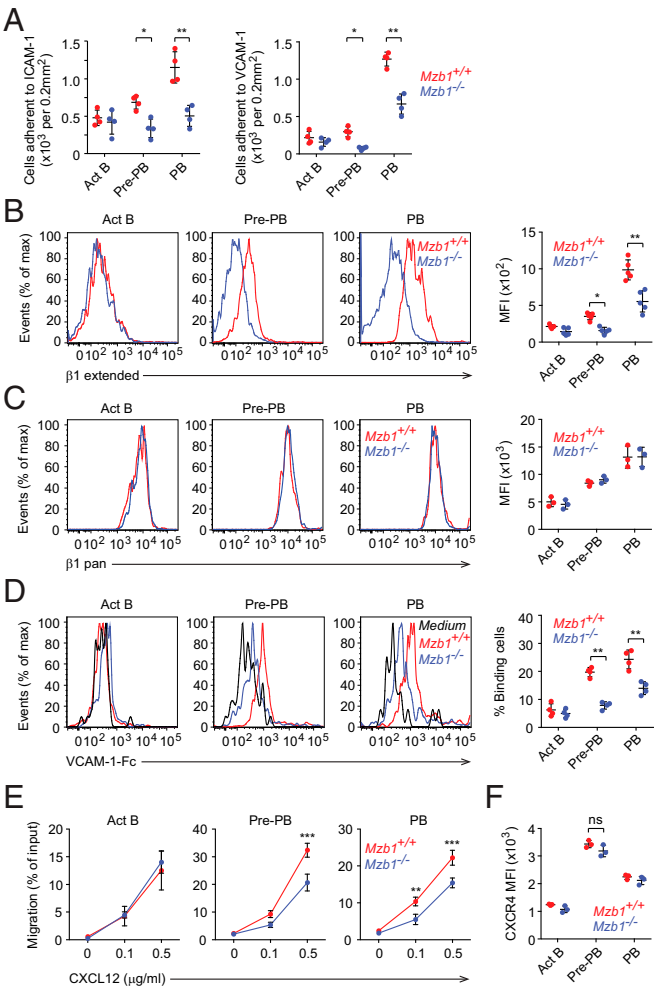

Fig. 4. *Mzb1*$^{-/-}$ ASCs show impaired β1 integrin activation and migration. (*A*) Adhesion of Act B, Pre-PB, and PB cells to slides coated with ICAM-1 (*Left*) or VCAM-1 (*Right*). (*B* and *C*) Representative histograms and quantification (mean fluorescent intensity, MFI) of extended β1-integrin (*B*) and total β1-integrin (β1 pan) in Act B, Pre-PB, and PB cells. Data are representative of three experiments; $n = 3$. (*D*) Representative histograms showing the adhesion of Act B, pre-PB and PB cells to soluble VCAM-1, and quantification of the frequency of the binding cells. (*E*) Transwell assay to assess the migration of Act B, Pre-PB, and PB cells toward CXCL12 (0, 0.1 and 0.5 μg/mL) on VCAM-1–coated plates. (*F*) Quantification (MFI) of CXCR4 cell surface expression in the corresponding cells. ns, nonsignificant. Data are representative of three independent experiments. $n = 3$. *$P < 0.05$, **$P < 0.01$, ***$P < 0.001$.

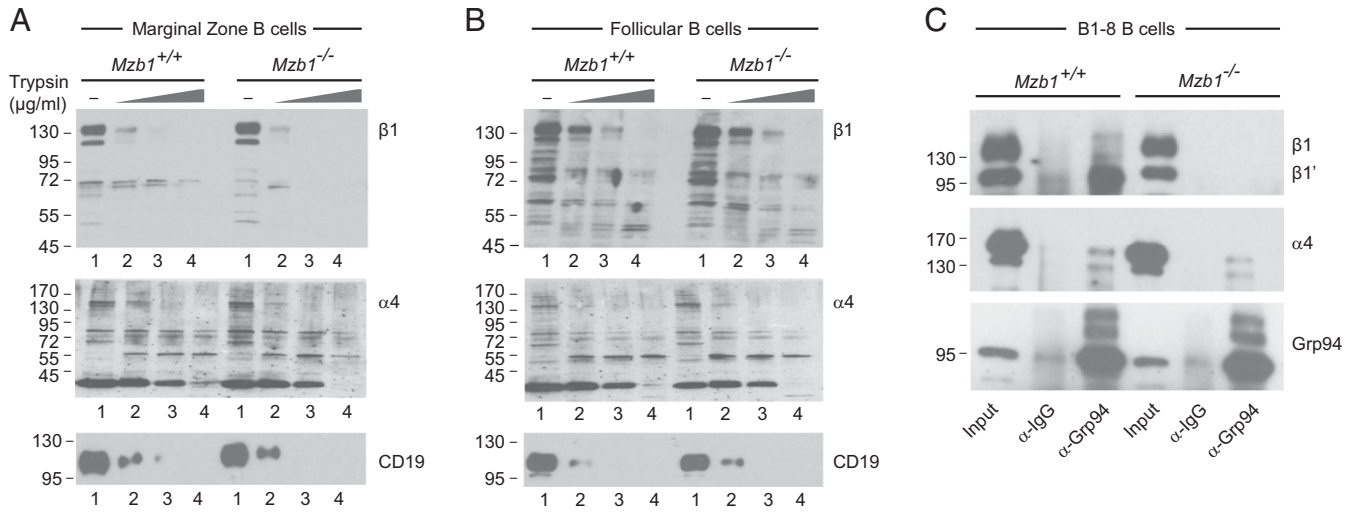

Fig. 5. Analysis of the conformation of α4- and β1-integrins in $Mzb1^{+/+}$ and $Mzb1^{-/-}$ MZ B cells (*A*) and Fo B cells (*B*) by limited proteolysis. Cells were lysed and increasing concentrations of trypsin (0, 25, 50, and 100 μg/mL; lanes 1, 2, 3, and 4, respectively) were added. CD19 was used as control. Sample buffer was used to stop proteolysis and samples were resolved by SDS/PAGE. Western blotting was performed and protease-resistant fragments were detected by specific antibodies. (*C*) Coimmunoprecipitation to detect the association of Grp94 with α4- and β1-integrins. Lysates of $Mzb1^{+/+}$ and $Mzb1^{-/-}$ B1-8 B cells were incubated with beads cross-linked with α-Grp94 or control α-Ig antibodies. Samples were washed and resolved by SDS/PAGE. Grp94, β1-, and α4-integrins were detected by immunoblot analysis with specific antibodies. Data are representative of three different experiments.

data indicate that the Grp94 cochaperone Mzb1 is required for proper β1-integrin activation and function, consistent with previous identification of integrins as substrate-specific clients of the Grp94/gp96 chaperone (30).

Mzb1 Is Required for the Trafficking and Maintenance of BM PCs. The deficiency in integrin-mediated cell adhesion and the reduced frequency of $CD138^+$ $Blimp1^+$ ASCs in the BM raised the question of whether Mzb1 controls the trafficking of long-lived PCs to the BM niche. Homing of B cells and progenitor cells depends on the interaction of integrin α4β1 and BM-expressed VCAM-1, and this interaction is also considered crucial for the homing and survival of ASCs (31–33). To address whether Mzb1-controlled integrin activation regulates the trafficking of PBs to the BM, we performed several experiments. First, sorted $Mzb1^{-/-}$ and $Mzb1^{+/+}$ pre-PBs and PBs from LPS-stimulated splenic B cell cultures were differentially dye-labeled and transferred in a 1:1 ratio into nonirradiated WT mice. Twenty hours after the adoptive transfer, the ratio of $Mzb1^{+/+}$ to $Mzb1^{-/-}$ pre-PBs and PBs was not significantly changed in the spleen. However, the ratio of $Mzb1^{+/+}$ to $Mzb1^{-/-}$ PBs, which have arrived in the BM, was significantly shifted (*SI Appendix*, Fig. S3). Second, $B220^{low}CD138^+$ ASCs were sorted from $Mzb1^{+/+}$ and $Mzb1^{-/-}$ mice 3 dpi with TNP-LPS. These $Mzb1^{+/+}$ and $Mzb1^{-/-}$ ASCs were differentially dye-labeled and transferred in a 1:1 ratio into nonirradiated WT recipients. As a control, we also labeled and used $B220^+CD138^-$ splenic B cells. After 20 h, we found a similar ratio to control cells ($B220^+CD138^-$) in the spleen; however, in the BM, $Mzb1^{+/+}$ ASCs were found in a higher proportion than $Mzb1^{-/-}$ ASCs (Fig. 6 *A* and *B*). Third, we performed adoptive transfers with 1:1 mixtures of CD45.1 total WT BM with BM from either CD45.2 $Mzb1^{-/-}$ or CD45.2 $Mzb1^{+/+}$ mice. Ten weeks after adoptive transfer, chimeras were immunized with TNP-LPS and spleen and BM were analyzed 3 dpi. The numbers of Ag-IgM^+–specific cells in the spleen were similar between WT and $Mzb1^{-/-}$ mice, but they were significantly reduced in the BM of the $Mzb1^{-/-}$ mice (Fig. 6 *D* and *E*). Taken together, these experiments show that Mzb1-deficient PBs and ASCs are impaired in their trafficking to the BM, a cell-intrinsic defect that is not due to changes in the microenvironment.

Mzb1-Dependent Integrin Activation Is Required for PC Differentiation. To examine whether α4β1-mediated binding to VCAM-1 influences PB differentiation in vitro, we cultured splenic $B220^+$ cells on plates coated with increasing concentrations of VCAM-1 and induced their differentiation with LPS. We observed that VCAM-1 binding augmented the differentiation of $Mzb1^{+/+}$ $Prdm1^{+/gfp}$ B cells into $CD138^+Blimp1\text{-}GFP^+$ PBs. In contrast, the differentiation of $Mzb1^{-/-}Prdm1^{+/gfp}$ splenic B cells was not significantly increased by the exposure to VCAM-1 (Fig. 6*C*, *Upper*). Importantly, this difference between $Mzb1^{+/+}$ and $Mzb1^{-/-}$ PB differentiation was further augmented in the presence of CXCL12 when β1-integrin activation was induced (Fig. 6*C*, *Lower*). These data suggest that the activation of integrins promotes PC differentiation in vitro.

To test our hypothesis that Mzb1-dependent integrin activation and binding to VCAM-1 influences PB differentiation, we examined whether the blocking of VCAM-1 function in vivo would mimic the Mzb1-deficiency. To this end, we immunized $Mzb1^{+/+}Prdm1^{+/gfp}$ and $Mzb1^{-/-}Prdm1^{+/gfp}$ mice with TNP-LPS and administered intravenously anti–VCAM-1 or IgG control antibody 24 h later. The frequencies of $CD138^+Blimp^{int}$ PBs remained virtually unchanged under all conditions. However, the blocking of VCAM-1 in immunized $Mzb1^{+/+}Prdm1^{+/gfp}$ control mice lead to a significant drop of splenic $CD138^+Blimp^{hi}$ PC frequencies relative to the frequencies of these cells in IgG-treated *Mzb1* knockout animals (Fig. 7 *A* and *B*). Moreover, VCAM-1 blocking in $Mzb1^{-/-}Prdm1^{+/gfp}$ mice did not further lower the frequencies of splenic $CD138^+Blimp^{hi}$ PCs (Fig. 7 *A* and *B*). These specific effects of anti–VCAM-1 treatment were also reflected in the generation of TNP-specific ASCs in ELISpot assays (Fig. 7*C*). Importantly, the same effects of VCAM-1–blocking were also measured for $CD138^+Blimp^{hi}$ PC frequencies in the BM (Fig. 7 *D*–*F*).

Discussion

By analyzing the generation and function of PCs in $Mzb1^{-/-}$ $Prdm1^{+/gfp}$ and $Mzb1^{+/+}Prdm1^{+/gfp}$ mice, we found that Mzb1

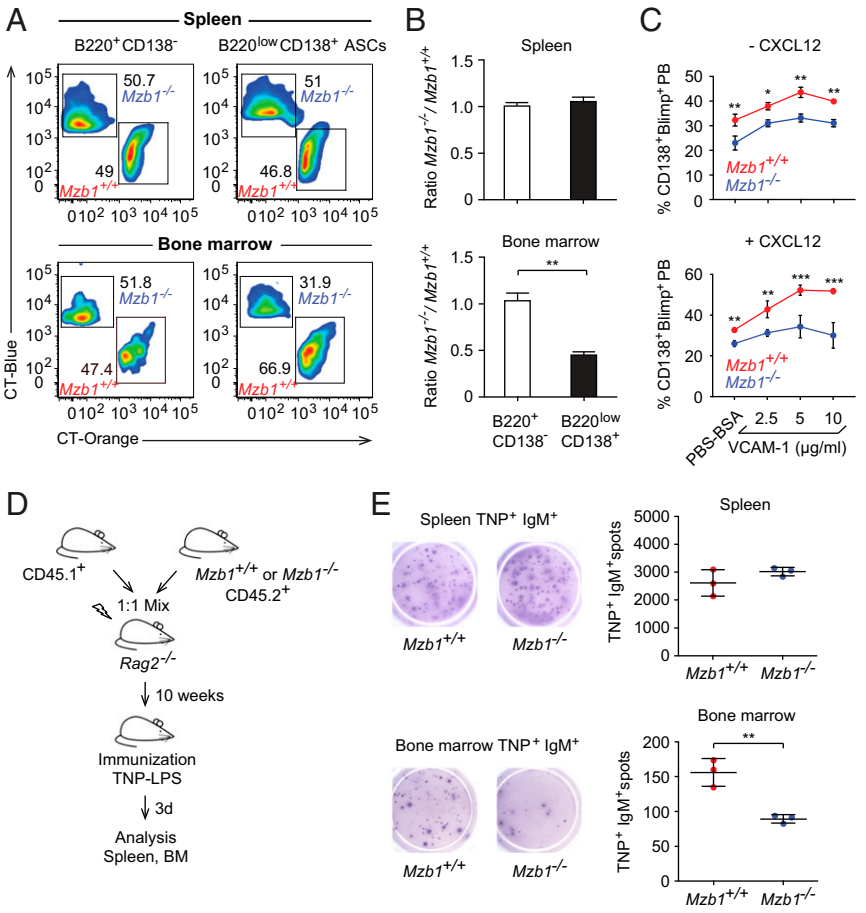

Fig. 6. (*A*) Flow cytometric analysis to detect CT orange-labeled *Mzb1*$^{+/+}$ B220^{low}CD138^{+} ASCs and CT blue-labeled *Mzb1*$^{-/-}$ ASCs from TNP-LPS-immunized mice that have been sorted, labeled, and transferred in a 1:1 ratio into recipient mice 20 h before flow cytometric analysis. B220^{+}CD138^{-} cells served as a control. Numbers represent cell frequencies. (*B*) Ratios (±SD) between *Mzb1*$^{-/-}$ and *Mzb1*$^{+/+}$ B220^{low}CD138^{+} ASCs that migrated to the spleen and BM. Data represent two independent experiments; $n = 3$. (*C*) Frequencies of CD138^{+}Blimp-GFP^{+} PBs in cultures of LPS-stimulated B220 splenocytes of *Mzb1*$^{+/+}$*Prdm1*$^{+/gfp}$ and *Mzb1*$^{-/-}$*Prdm1*$^{+/gfp}$ mice on VCAM-1–coated plates, in the absence (*Upper*) or presence (*Lower*) of CXCL12. Frequencies of CD138^{+}Blimp-GFP^{+} PBs (±SD) from three different experiments are shown. $n = 3$. $^{*}P < 0.05$, $^{**}P < 0.01$, $^{***}P < 0.001$. (*D*) Schematic representation of mixed BM chimeras. BM from either CD45.2^{+} *Mzb1*$^{+/+}$ or CD45.2^{+} *Mzb1*$^{-/-}$ were mixed 1:1 with BM from CD45.1^{+} mice and transferred into irradiated *Rag2*$^{-/-}$ mice. Ten weeks after transfer, the recipient mice were immunized with TNP-LPS, and analyzed 3 d after. (*E*) Representative ELISpot (*Left*) and mean (±SD) numbers (*Right*) of TNP^{+}IgM^{+} ASCs in spleen (*Upper*) and BM (*Lower*) 3 dpi of the mixed BM chimeras; $n = 4$. Data are representative of two different experiments with three to six mice per group and experiment. $^{**}P < 0.01$.

plays a role not only in the secretion of antibody but also in the differentiation and migration of PCs. Mzb1 functions as an ER-localized cochaperone of Grp94/gp96, which has a limited set of client proteins, including Ig, TLRs, and integrins (13, 30, 34). TLR-4 expression is normal in Mzb1-deficient mice (13) but it is impaired in mice deficient in the Grp94/gp96 cochaperone Cnpy3/Prat4a (35–37). Consistent with the abundant expression of Mzb1 in MZ B and peritoneal B1 B cells, we show that Mzb1 is required for the generation of PCs specifically in a TI humoral immune response. Blimp1 is known to be required both for the initial differentiation of ASCs and for the production of antibody by existing ASCs (8, 9). Given that Blimp1 is also a direct activator of *Mzb1* expression (8), it is noteworthy that the defect in the generation of *Mzb1*$^{-/-}$ PBs in vitro resembles, at least in part, that of Blimp1-deficient PBs. The resemblance of phenotypes suggests that Mzb1 is a functionally important target of Blimp1 in ASCs that ultimately influences Blimp1 function in a feedback loop. This feedback loop could occur through an indirect role of Mzb1 in enhancing the function of Blimp1 or a Blimp1-cooperating protein, whereby Mzb1 would facilitate the folding or function of a cell surface or secreted protein that regulates Blimp1.

Mzb1 regulates the folding of β1-integrin in the ER as evidenced by the reduced reactivity of Mzb1-deficient cells toward a conformation-specific antibody and the enhanced sensitivity toward proteolysis. Consistent with the localization of Mzb1 in the ER, an intracellular organelle that provides a proper environment for membrane and secretory proteins to attain a 3D functional conformation (38), we find that Mzb1 is required for the association of Grp94 with the ER-form of β1-integrin. Previous kinetic analysis of β1-integrin folding indicated that newly synthesized β1-integrins acquire their native conformation early in the ER before the assembly with α-integrins and exit from the ER (16, 29). The ER-form of monomeric β1-integrin, termed β1′, is in an extended conformation that requires a disulphide within a small cysteine-rich stretch (29). β1′-Integrin is the precursor of the mature β1 Golgi form, which is associated with an α-subunit. The β1-subunit of the α/β heterodimer exhibits an inactive (bent) conformation throughout intracellular trafficking until a reduction of the Ca^{2+} concentration, addition of extracellular Mn^{2+}, ligand binding, or chemokine-mediated inside-out signaling induces the active (extended) conformation of the β1-subunit on the cell surface (16, 27, 29). In addition to enhancing the interaction of Grp94 with specific substrates, Mzb1 also

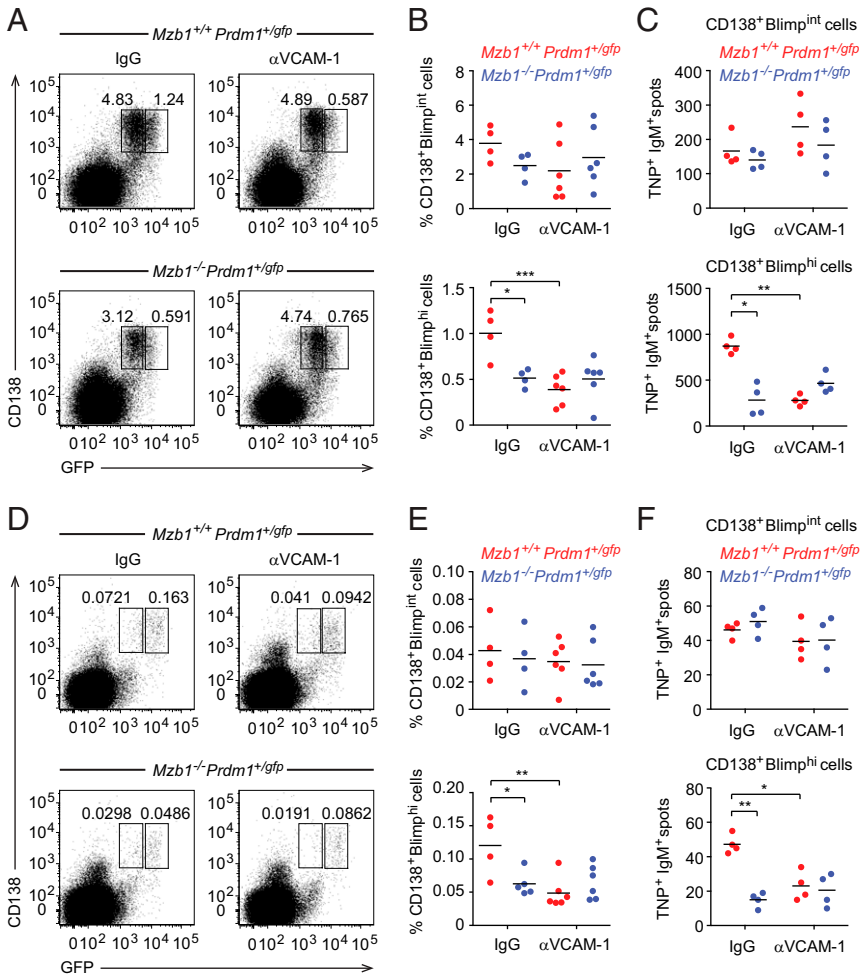

Fig. 7. Role of VCAM-1–mediated β1-integrin activation in PC differentiation. (*A* and *B*) Flow cytometry to identify CD138$^+$Blimp-GFP^{int} PB and CD138$^+$Blimp-GFP^{hi} PC in spleen of *Mzb1*$^{+/+}$*Prdm1*$^{+/gfp}$ and *Mzb1*$^{-/-}$*Prdm1*$^{+/gfp}$ mice that were administered 100 μg of anti–VCAM-1 antibody or rat IgG intravenously 24 h after TNP-LPS immunization and 2 d before analysis. (*B*) Mean (±SD) frequencies of PB (*Upper*) and PC (*Lower*). (*C*) ELISpot analysis to detect TNP$^+$IgM$^+$ -secreting PB and PC cells in spleen. Data are representative of three different experiments; $n = 4$–6. *$P < 0.05$, **$P < 0.01$, ***$P < 0.001$. (*D*–*F*) Flow cytometry and ELISpot analysis to detect CD138$^+$Blimp-GFP^{int} PB and CD138$^+$Blimp-GFP^{hi} PC in the BM of TNP-LPS–immunized and anti–VCAM-1–treated *Mzb1*$^{+/+}$*Prdm1*$^{+/gfp}$ and *Mzb1*$^{-/-}$*Prdm1*$^{+/gfp}$ mice as in *A*–*C*.

interacts with the sarco/ER Ca^{2+}-ATPase (SERCA) pump and influences the intracellular Ca^{2+} concentration (12, 13). Thus, Mzb1 may help monomeric β1-integrin to acquire an activation-competent conformation in the ER. In the absence of Mzb1, β1-integrin may have a partial defect in the proper folding of the cysteine-rich stretch that is recognized by the conformation-sensitive 9EG7 antibody but it will not interfere with the formation of α/β-integrin that is displayed on the cell surface. Although generally misfolded proteins do not reach the cell surface, partially misfolded proteins can exit the ER and are detected on the cell surface as shown for the LDL receptor (39).

A role of α4β1-integrin in PBs can be inferred from the impaired differentiation in vitro and in mice that have been treated with anti–VCAM-1 antibody. Mzb1-dependent integrin activation may also be required for the trafficking of ASCs to the BM, which has been shown to involve a CXCL12 chemokine gradient (31). The impaired integrin activation in Mzb1-deficient ASCs may account for their reduced migration toward the chemokine CXCL12. *Mzb1*$^{-/-}$ ASCs express normal levels of CXCR4 receptor on the cell surface, suggesting that the migration defect is due to an impaired β1-integrin activation rather than an impaired chemokine sensing. Reduced migration of cells toward CXCL12 despite normal CXCR4 surface expression has also been observed in other studies (40–43). Trafficking defects of ASCs have often been associated with their mislocalization in spleen (32, 43, 44). Therefore, these cells may have a defect in exiting the spleen, resulting in a reduced frequency of PCs in the BM. In conclusion, our study provides insight into the role of Mzb1 in regulating the differentiation and trafficking of PCs via facilitating the activation of integrins.

Materials and Methods

Mice. All mouse experiments were carried out in accordance to the guidelines of the Federation of European Laboratory Animal Science Association and following legal approval of the Regierungspräsidium Freiburg. *Mzb1*$^{+/+}$ and *Mzb1*$^{-/-}$ mice were generated as previously described (13). *Prdm1*$^{+/gfp}$ mice were obtained from the laboratory of S.L.N. Mouse strains were bred and maintained in the Max Planck Institute of Immunobiology and Epigenetics Freiburg's conventional animal care facility. Experiments were performed in 6- to 12-wk-old mice from C57BL/6J background.

Flow Cytometry. Single-cell suspensions were resuspended in PBS 2% FCS and stained for flow cytometric analysis. Data were acquired with a LSR Fortessa (BD Biosciences) and analyzed using FlowJo software. Antibodies against the following molecules were used: CD19 (6D5), CD93 (AA4.1), CD23 (B3B4), GL7 (GL-7), CD184 (CXCR4-2B11) from eBioscience; CD21 (7G6), B220 (RA3-6B2), CD138 (281-2), CD45.1 (A20), CD45.2 (104), IgM (R6-60.2), Fas (Jo2) from

BD. Anti-CD29 (9EG7) in combination with secondary anti-rat PE antibody (both BD) was used to detect the active conformation state of β1-integrin. Anti-CD29 (HMb1-1) antibody was used to detect the total (pan) β1-integrin (eBioscience). IgG1 biotinylated antibody (Southern Biotech) was conjugated with SA-BV421 (Biolegend). NP-PE antibody was from Biosearch Tech. Anti-CD16/32 (93) (BD) was used to block nonspecific binding.

Immunizations, ELISpot, and Antibody Treatments. Mice were injected intraperitoneally with 50 μg TNP-LPS, 50 μg NP-Ficoll, or 150 μg adsorbed NP-KLH (Biosearch Technology) 1:1 ratio onto Alu-Gel-S (Serva). Spleens, BM, and blood were taken after the indicated time points postimmunization. ASCs were analyzed by ELISpot as previously described (13). In some experiments, mice received 100 μg of anti–VCAM-1 (429) or rat IgG2a isotype control antibodies (both BD), intravenously, 24 h postinfection. Spleens and BM were analyzed 48 h after antibody treatment.

Apoptosis Assay. ASCs ($B220^{low}CD138^{+}$) from *Mzb1*$^{+/+}$ and *Mzb1*$^{-/-}$ mice were stained for Annexin V-FITC and 7AAD, according to the protocol's instructions (BD Bioscience) 3 dpi with TNP-LPS. Cells were acquired in LSR Fortessa flow cytometer and analyzed with FlowJo software.

BM Chimeras. For 50:50 BM chimeras, lethally irradiated *Rag2*$^{-/-}$ mice (2 × 6 Gy) were reconstituted in an equal ratio with CD45.1 C57BL6/J and either CD45.2 *Mzb1*$^{+/+}$ BM or CD45.2 *Mzb1*$^{-/-}$ BM. Mice were rested for 10 wk before TNP-LPS immunization.

Adoptive Transfer. *Mzb1*$^{+/+}$ and *Mzb1*$^{-/-}$ ASCs ($B220^{low}CD138^{+}$) or control $B220^{+}CD138^{-}$ were sorted 3 dpi with TNP-LPS, and were incubated with 0.5 μM Cell Tracker (CT) Orange or 1 μM CT Blue (Molecular Probes), respectively, at 37 °C for 30 min. Cells were washed and mixed in a 1:1 ratio for intravenous injection in C57BL/6 recipient mice. A total of 1×10^5 cells/100 μL were injected per tail vein. Labeled cells from spleens and BM of recipient mice were analyzed by flow cytometer 20 h after adoptive transfer. The same experiment was performed with $CD138^{-}$ $Blimp^{+}$ (Pre-PB) and $CD138^{+}$ $Blimp^{+}$ (PB) differentiated from splenic $B220^{+}$ cells of *Mzb1*$^{+/+}$*Prdm1*$^{+/gfp}$ and *Mzb1*$^{-/-}$*Prdm1*$^{+/gfp}$ mice.

In Vitro Differentiation of PBs. To mimic TI immunization in vitro, splenic B cells were purified from *Mzb1*$^{+/+}$ and *Mzb1*$^{-/-}$*Prdm1*$^{+/gfp}$ mice using anti-B220 magnetic beads (Miltenyi Biotec) and cultured with 25 μg/mL LPS (L5668; Sigma-Aldrich). After 4 d, three populations were isolated: $CD138^{-}$ $Blimp^{-}$ activated B (Act B) cells, $CD138^{-}$ $Blimp^{+}$ (Pre-PB), and $CD138^{+}Blimp^{+}$ (PB). In some experiments cells were differentiated in 96-U–bottom-well plates, coated overnight at 4 °C with VCAM-1 (2.5, 5 and 10 μg/mL; R&D Systems). After coating, plates were washed and blocked with Iscove's modified Dulbecco's medium (IMDM)-BSA 1% for 1 h at 37 °C. $B220^{+}$ cells (1×10^5) were added to the wells and cultured with LPS, in the absence or presence of recombinant CXCL12 (0.5 μg/mL; R&D Systems). To differentiate $CD138^{+}Blimp^{+}$ cells under TD conditions, $B220^{+}$ cells were cultured for 5 d in the presence of CD40L (5 ng/mL), IL-4, and IL-5 (10 ng/mL; Peprotech).

mRNA Preparation and RNA-Seq Analysis. In vitro differentiated Act B, Pre-PB, and PB cells were sorted by flow cytometry (FACSAria; Becton Dickinson) and total RNA was isolated with an RNeasy Mini Kit (Qiagen) and treated with DNase I, according to the manufacturer's instructions. The total mRNA was enriched by Oligo-dT magnetic beads. The libraries were prepared by using a TruSeq Stranded mRNA library preparation kit. The samples were sequenced using Illumina HiSEq. 3000. The base calling was performed by using BCL2Fastq pipeline (v0.3.1) and bcl2fastq (v2.17.1.14). The paired-end RNA-Seq datasets were mapped to the mouse reference genome (mm9) using Tophat (v2.0.14) and Bowtie (v2.2.6.0) (45). The mapped reads were further assembled by using Cufflinks (v2.2.1). The expression level of the annotated genes (Univerisity of California, Santa Cruz, mm9) was calculated by Cuffquant (46). The two biological replicates of each condition were normalized and the differential gene expression between the conditions was calculated by using Cuffdiff. The gene sets were further filtered for more than twofold up- or down-regulation. The RNA-Seq profile of the Mzb1 locus was visualized by using MISO (47). The differentially expressed genes were curated using gene ontology, panther functional classifications, and the published literature (8, 9).

Transwell Migration Assay. Act B, Pre-PB, and PB were sorted by flow cytometry (as described above). Next, 1×10^5 cells (100 μL) were placed in the upper compartment, and IMDM medium (200 μL) containing recombinant CXCL12 (0, 0.1 or 0.5 μg/mL) (SDF-1α; R&D Systems) was placed in the lower compartment of VCAM-1 (5 μg/mL in PBS; R&D Systems) -coated transwell chamber (5-μm pore size; Corning). After incubation at 37 °C for 4 h, cells migrating into the lower chamber were counted by collecting events for a fixed time (60 s) on a LSR Fortessa flow cytometer, and their percentage relative to the total cells was calculated.

Static Adhesion Assay and VLA-4 Affinity Assay. Adhesion assays and a VLA-4 affinity assay was performed, as previously described (12).

Limited Proteolysis. Limited proteolysis was carried out as previously described (48). MZ and Fo B cells were lysed in 1% Triton X-100, 10 mM Hepes pH 7.4, and 150 mM NaCl. Following nuclei pelleting, protein amount was quantified and supernatant containing equal protein amounts was divided into aliquots, and trypsin was added in increasing concentrations (0, 25, 50, and 100 μg/mL) for 15 min. Proteolysis was stopped using sample buffer. DTT was added to the samples to achieve a final concentration of 25 mM. Digested samples were heated for 5 min at 95 °C, resolved by SDS/PAGE and immunoblotted with β1-integrin (183666; Abcam), α4-integrin (8440; Cell Signaling), and CD19 (3574; Cell Signaling) antibodies.

Coimmunoprecipitation. B1-8 B cells were lysed in 2% CHAPS (C3023; Sigma), 10 mM Hepes pH 7.4, and 150 mM NaCl, 1 mM PMSF, and protease inhibitor mixture (P8340; Sigma). Precleared lysates were transferred to Sepharose beads (GE Healthcare) preincubated for 2 h at 4 °C with rabbit polyclonal Grp94 (ab13509; Abcam) or IgG control (2729; Cell Signaling) antibodies. After 4 h, immunoprecipitates were washed and resuspended in sample buffer with DTT (25 mM). Samples were heated for 5 min at 95 °C and resolved by SDS/PAGE. After electrophoresis, samples were transferred onto an nitrocellulose membrane, and immunoblotted with β1-integrin (183666; Abcam) and α4-integrin (8440; Cell Signaling) antibodies.

Statistics. Data are expressed as mean ± SD. Data were analyzed by two-tailed Student's *t* test or one-way ANOVA as appropriate, using the GraphPad Prism program (v7). *P* values of less than 0.05, 0.01, and 0.001 were considered significant.

Data Deposition. The RNA-seq data reported in this paper have been deposited to the National Center for Biotechnology Gene Expression Omnibus (GEO) database (accession no. GSE118124).

ACKNOWLEDGMENTS. We thank Eirini Trompouki for critical reading the manuscript; Marika Rott for the assistance with the manuscript preparation; Ingrid Falk and Franziska Ludin for technical assistance; members of R.G.'s department for the discussions; and the Deep Sequencing, Flow Cytometry Facility, and Mouse facilities of the Max Planck Institute. This work was supported by funds from the Max Planck Society and German Research Foundation.

1. Shapiro-Shelef M, Calame K (2005) Regulation of plasma-cell development. *Nat Rev Immunol* 5:230–242.
2. Nutt SL, Hodgkin PD, Tarlinton DM, Corcoran LM (2015) The generation of antibody-secreting plasma cells. *Nat Rev Immunol* 15:160–171.
3. Allman D, Pillai S (2008) Peripheral B cell subsets. *Curr Opin Immunol* 20:149–157.
4. Cerutti A, Cols M, Puga I (2013) Marginal zone B cells: Virtues of innate-like antibody-producing lymphocytes. *Nat Rev Immunol* 13:118–132.
5. Todd DJ, Lee AH, Glimcher LH (2008) The endoplasmic reticulum stress response in immunity and autoimmunity. *Nat Rev Immunol* 8:663–674.
6. Walter P, Ron D (2011) The unfolded protein response: From stress pathway to homeostatic regulation. *Science* 334:1081–1086.
7. Kallies A, et al. (2007) Initiation of plasma-cell differentiation is independent of the transcription factor Blimp-1. *Immunity* 26:555–566.
8. Minnich M, et al. (2016) Multifunctional role of the transcription factor Blimp-1 in coordinating plasma cell differentiation. *Nat Immunol* 17:331–343.
9. Tellier J, et al. (2016) Blimp-1 controls plasma cell function through the regulation of immunoglobulin secretion and the unfolded protein response. *Nat Immunol* 17: 323–330.
10. Shimizu Y, Meunier L, Hendershot LM (2009) pERp1 is significantly up-regulated during plasma cell differentiation and contributes to the oxidative folding of immunoglobulin. *Proc Natl Acad Sci USA* 106:17013–17018.
11. van Anken E, et al. (2009) Efficient IgM assembly and secretion require the plasma cell induced endoplasmic reticulum protein pERp1. *Proc Natl Acad Sci USA* 106: 17019–17024.
12. Flach H, et al. (2010) Mzb1 protein regulates calcium homeostasis, antibody secretion, and integrin activation in innate-like B cells. *Immunity* 33:723–735.

13. Rosenbaum M, et al. (2014) MZB1 is a GRP94 cochaperone that enables proper immunoglobulin heavy chain biosynthesis upon ER stress. *Genes Dev* 28:1165–1178.
14. Shi W, et al. (2015) Transcriptional profiling of mouse B cell terminal differentiation defines a signature for antibody-secreting plasma cells. *Nat Immunol* 16:663–673.
15. Kinashi T (2005) Intracellular signalling controlling integrin activation in lymphocytes. *Nat Rev Immunol* 5:546–559.
16. Luo BH, Carman CV, Springer TA (2007) Structural basis of integrin regulation and signaling. *Annu Rev Immunol* 25:619–647.
17. Lu TT, Cyster JG (2002) Integrin-mediated long-term B cell retention in the splenic marginal zone. *Science* 297:409–412.
18. Ulyanova T, et al. (2005) VCAM-1 expression in adult hematopoietic and non-hematopoietic cells is controlled by tissue-inductive signals and reflects their developmental origin. *Blood* 106:86–94.
19. Jacobsen K, Kravitz J, Kincade PW, Osmond DG (1996) Adhesion receptors on bone marrow stromal cells: In vivo expression of vascular cell adhesion molecule-1 by reticular cells and sinusoidal endothelium in normal and gamma-irradiated mice. *Blood* 87:73–82.
20. Koni PA, et al. (2001) Conditional vascular cell adhesion molecule 1 deletion in mice: Impaired lymphocyte migration to bone marrow. *J Exp Med* 193:741–754.
21. Leuker CE, Labow M, Müller W, Wagner N (2001) Neonatally induced inactivation of the vascular cell adhesion molecule 1 gene impairs B cell localization and T cell-dependent humoral immune response. *J Exp Med* 193:755–768.
22. Minges Wols HA, Underhill GH, Kansas GS, Witte PL (2002) The role of bone marrow-derived stromal cells in the maintenance of plasma cell longevity. *J Immunol* 169: 4213–4221.
23. Tokoyoda K, Egawa T, Sugiyama T, Choi BI, Nagasawa T (2004) Cellular niches controlling B lymphocyte behavior within bone marrow during development. *Immunity* 20:707–718.
24. Kallies A, et al. (2004) Plasma cell ontogeny defined by quantitative changes in blimp-1 expression. *J Exp Med* 200:967–977.
25. Taubenheim N, et al. (2012) High rate of antibody secretion is not integral to plasma cell differentiation as revealed by XBP-1 deficiency. *J Immunol* 189:3328–3338.
26. Lenter M, et al. (1993) A monoclonal antibody against an activation epitope on mouse integrin chain beta 1 blocks adhesion of lymphocytes to the endothelial integrin alpha 6 beta 1. *Proc Natl Acad Sci USA* 90:9051–9055.
27. Bazzoni G, Shih DT, Buck CA, Hemler ME (1995) Monoclonal antibody 9EG7 defines a novel beta 1 integrin epitope induced by soluble ligand and manganese, but inhibited by calcium. *J Biol Chem* 270:25570–25577.
28. Fagarasan S, Honjo T (2000) T-independent immune response: New aspects of B cell biology. *Science* 290:89–92.
29. Tiwari S, Askari JA, Humphries MJ, Bulleid NJ (2011) Divalent cations regulate the folding and activation status of integrins during their intracellular trafficking. *J Cell Sci* 124:1672–1680.
30. Staron M, et al. (2010) gp96, an endoplasmic reticulum master chaperone for integrins and Toll-like receptors, selectively regulates early T and B lymphopoiesis. *Blood* 115:2380–2390.
31. Cyster JG (2003) Homing of antibody secreting cells. *Immunol Rev* 194:48–60.
32. Li YF, Xu S, Ou X, Lam KP (2014) Shp1 signalling is required to establish the long-lived bone marrow plasma cell pool. *Nat Commun* 5:4273.
33. van Spriel AB, et al. (2012) The tetraspanin CD37 orchestrates the α(4)β(1) integrin-Akt signaling axis and supports long-lived plasma cell survival. *Sci Signal* 5:ra82.
34. Ansa-Addo EA, et al. (2016) Clients and oncogenic roles of molecular chaperone gp96/grp94. *Curr Top Med Chem* 16:2765–2778.
35. Liu B, et al. (2010) Folding of Toll-like receptors by the HSP90 paralogue gp96 requires a substrate-specific cochaperone. *Nat Commun* 1:79.
36. Takahashi K, et al. (2007) A protein associated with Toll-like receptor (TLR) 4 (PRAT4A) is required for TLR-dependent immune responses. *J Exp Med* 204:2963–2976.
37. Wakabayashi Y, et al. (2006) A protein associated with toll-like receptor 4 (PRAT4A) regulates cell surface expression of TLR4. *J Immunol* 177:1772–1779.
38. Braakman I, Bulleid NJ (2011) Protein folding and modification in the mammalian endoplasmic reticulum. *Annu Rev Biochem* 80:71–99.
39. Pena F, Jansens A, van Zadelhoff G, Braakman I (2010) Calcium as a crucial cofactor for low density lipoprotein receptor folding in the endoplasmic reticulum. *J Biol Chem* 285:8656–8664.
40. Wehrli N, et al. (2001) Changing responsiveness to chemokines allows medullary plasmablasts to leave lymph nodes. *Eur J Immunol* 31:609–616.
41. Hauser AE, et al. (2002) Chemotactic responsiveness toward ligands for CXCR3 and CXCR4 is regulated on plasma blasts during the time course of a memory immune response. *J Immunol* 169:1277–1282.
42. Kabashima K, et al. (2006) Plasma cell S1P1 expression determines secondary lymphoid organ retention versus bone marrow tropism. *J Exp Med* 203:2683–2690.
43. Good-Jacobson KL, O'Donnell K, Belz GT, Nutt SL, Tarlinton DM (2015) c-Myb is required for plasma cell migration to bone marrow after immunization or infection. *J Exp Med* 212:1001–1009.
44. Hargreaves DC, et al. (2001) A coordinated change in chemokine responsiveness guides plasma cell movements. *J Exp Med* 194:45–56.
45. Kim D, et al. (2013) TopHat2: Accurate alignment of transcriptomes in the presence of insertions, deletions and gene fusions. *Genome Biol* 14:R36.
46. Trapnell C, et al. (2013) Differential analysis of gene regulation at transcript resolution with RNA-seq. *Nat Biotechnol* 31:46–53.
47. Katz Y, Wang ET, Airoldi EM, Burge CB (2010) Analysis and design of RNA sequencing experiments for identifying isoform regulation. *Nat Methods* 7:1009–1015.
48. Thibodeau PH, et al. (2010) The cystic fibrosis-causing mutation deltaF508 affects multiple steps in cystic fibrosis transmembrane conductance regulator biogenesis. *J Biol Chem* 285:35825–35835.